Electrospun Nanofibers in Batteries

Subjects: Energy & Fuels

Contributor: Andrea Ehrmann

Electrospinning spinning techniques enables spinning continuous nanofibers with typical diameters in the range of some ten to some hundred nanometers. Rechargeable or secondary batteries are electrochemical power sources commonly utilized in portable devices such as camcorders, mobile phones, laptops, and electric transportations. In general, batteries are comprised of one or more electrochemical cells. Positive electrode (cathode), negative electrode (anode), porous separator membrane, and ionic conductive electrolyte are the essential components for fabrication of each electrochemical cell, electrospun fibers could enhanced various characteristics of electrolytic cells.

batteries Electrospun Nanofibers

1. Electrospinning Process

The electrospinning technique has been identified as a versatile and highly efficient method for fabrication of continuous nanofibers from polymer solution or melt. Generally, an electrospinning set-up contains a high voltage power supplier, a feeding pump, a spinning apparatus (such as spinneret), and a rotational/constant collector. In electrospinning procedure, ultrathin fibers are fabricated in an electrical field created between the collector and spinneret by applying a high voltage. The applied voltage, the distance between the spinneret and collector, the feeding rate, the spinneret inner diameter, and the collector speed belong to the common electrospinning parameters which can influence morphology of the electrospun membranes as well as fiber diameters. Fiber orientation, pore size distribution, and membrane porosity are significant morphology features of the electrospun membranes. Apparently, the morphology characteristics and fiber diameter should be tuned to obtain the most appropriate electrospun fibrous structure for the considered application [1][2][3]. As an example, fiber orientation may lead to production of an electrochemical biosensor with high sensitivity, while it can reduce ionic conductivity of an electrospun electrolyte applicable in lithium ion batteries [4][5].

Optimum electrospinning parameters should be determined for each polymer system as they vary from polymer to polymer. Overall, increasing the applied voltage up to a critical point causes formation of finer fibers due to more stretching of the electrospinning jet resulting from higher repulsion forces in it. On the other hand, thicker or beaded electrospun fibers can be obtained by exceeding the critical voltage as a result of higher velocity as well as smaller size of the Taylor cone [6]. The electrospinning distance should be recognized regarding the evaporation rate and deposition time of the electrospinning jet to gain a uniform membrane. A short electrospinning distance may lead to formation of ribbon-like nanofibers with large diameters, whereas thick fibers are fabricated through a high electrospinning distance [7]. In addition, a critical flow rate is essential to obtain homogenous and beadless

electrospun fibers. By increasing the feeding rate beyond the critical point, defective fibers with high diameters in a wide range and large pore sizes may be obtained [8]. Moreover, the receiver type and collector speed mainly influence the fibers' orientations and so the pore sizes. As the collector speed increases, fibers with higher orientation and less porosity and pore sizes are obtained [9].

Besides the apparatus adjustments, features of the polymer solution or melt influence the membrane morphology and fibers' diameter. The role of polymer solutions on various features of the electrospun membrane depends on their concentration, viscosity, and conductivity. Enhancement of the solution concentration up to a critical point provides more entanglement between the polymer chains which results in formation of beadless fibers with higher uniformity. Nevertheless, beaded and defective fibers can be obtained beyond the critical point due to drying of the polymer solution on the applied spinneret tip. Notably similar trends have been observed for the viscosity impact on the obtained electrospun fibers by numerous researchers. Furthermore, the electrospinning process highly depends on the Coulomb forces between the electrical field and accumulated charges on the solution surface. Therefore, a polymer solution with very low conductivity cannot be electrospun due to lack of charges which are essential for formation of the Taylor cone. In contrast, polymer solutions with conductivity beyond the critical point cannot also be processed because of spreading of the fibers in the electrospinning environment [10][11].

2. Electrospun Nanofibers in Batteries

Increasing progress in technology has forced researchers to design batteries with higher energy density, lighter weight, and more flexible structure. A basic LIB comprises of a lithium metal oxide electrode as cathode, a graphite-based anode, a porous polypropylene (PP) or polyethylene (PE) film as separator, and a lithium salt/solvent solution as electrolyte (Figure 2). Charge/discharge procedure of the LIBs is performed through chemical reactions. During the charge process, free lithium ions migrate from the cathode toward the anode, via diffusion into the ionic conductive electrolyte. Simultaneously, the electrons travel toward the anode through the external circuit and form LiC_6 compound in the anode material. Apparently, the reverse behavior takes place in the discharge step [12][13]. Over the past decades, most research in advanced development of LIBs has emphasized the use of electrospun fibers for fabrication of versatile and highly efficient components [14][15]. Recent progresses in the fabrication of electrospun cathode, anode, separator, and electrolyte are provided in the following section.

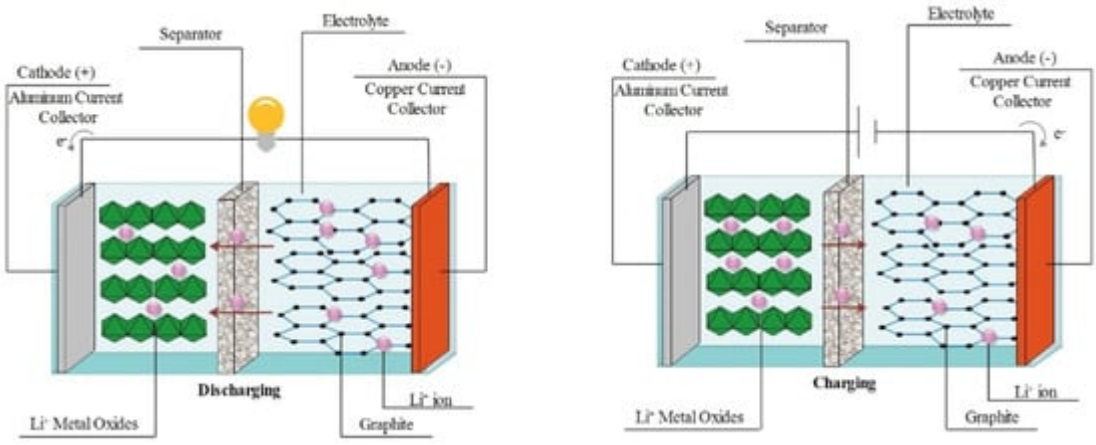

Figure 1. Schematic showing the intercalation mechanism in Li-ion batteries through charge and discharge. Reprinted from [16], with permission from Elsevier.

2.1. Electrospun Cathode Materials

Electrochemical performance of the batteries, such as potential window and storage capacity, is mostly affected by the cathode material. In fact, the number of extracted lithium ions from the cathode electrode determines the battery capacity. The energy could be stored in the cathode materials through two various conversion and intercalation techniques. In the conversion mechanism, lithium insertion and extraction are associated with changes in the crystalline structure of the applied cathode material, while the cathode structure acts as a host in the intercalation mechanism. So, the lithiation/delithiation can reversibly occur in the intercalation cathode materials. Notably, low electron conduction as well as high volume expansion have been reported as challenges linked with the conversion cathode materials. Therefore, the intercalation cathode structures have received more attention from numerous researchers. Among various types of intercalation structures (transition metal oxides, chalcogenides, and poly anions), transition metal oxides and poly-anionic compounds have displayed superior characteristics such as higher energy storage and greater operating voltage, while development of chalcogenide materials has been influenced by their irreversible structure [17][18].

Layered structures have been identified as the most widely applied electrode materials in the commercial LIBs. They are commonly presented by the chemical formula of $LiXO_2$, where X could be Co, Mn, or Ni. This group of cathode materials was first introduced by discovering of $LiCoO_2$ in the 1990s. During discharging, $LiCoO_2$ hexagonal cells are formed in layered structures, whereas $Li_{1-x}CoO_2$ monoclinic phases are created as a result of Li^+ ion removal during the charging procedure. The structural instability of $LiCoO_2$ cathode material is a major drawback associated with these materials which has resulted in lower practical capacity (140 $mAh{\cdot}g^{-1}$) compared with the reported theoretical capacity (280 $mAh{\cdot}g^{-1}$). So, $LiNiO_2$ was introduced to address the low experimental storage capacity. However, poor thermal stability, along with low electrochemical activity restricts practical usage of the layered $LiNiO_2$. Therefore, $LiNi_{0.5}Mn_{0.5}O_2$ was presented by Ohzuku et al. as a modified compound. Based on various analyses, this cathode material has revealed appropriate structural stability due to the existence of Mn^{4+} cations. In addition, it has represented a stable structure up to 300 °C, which is a crucial function for being applied in commercial batteries. Moreover, it has shown superior storage capacity (200 $mAh{\cdot}g^{-1}$) compared with the $LiCoO_2$ layered structure, although limitation of Li^+ ion extraction due to presence of Ni in the cathode material has caused synthesis and evaluation of $LiCo_xNi_yMn_{1-x-y}O_2$ ternary compound materials such as $LiCo_{1/3}Ni_{1/3}Mn_{1/3}O_2$ [16][19].

Spinel oxides with the general chemical formula of LiM_2O_4 (e.g., $LiMn_2O_4$) are another group of cathode materials. Compared with layered structures, they are safer and more affordable. Three-dimensional paths in such structures facilitate Li^+ ion diffusion and therefore enhance the rate capability. Nevertheless, capacity fading is a critical disadvantage associated with these materials. To overcome the aforementioned obstacle, doping mechanism has been widely reported to reduce Jahn-Teller active Mn^{3+} ions and thus to enhance the electrochemical characteristics. Mg, Ni, Cr, Al, and many more metal elements belong to the applied dopant materials. As an

example, $LiNi_{0.5}Mn_{1.5}O_4$ compound has illustrated superior rate capability and wider potential window compared with $LiMn_2O_4$ spinel oxide structure [20][21].

Poly-anionic compounds, with the general chemical structure of $(XO_4)^{3-}$ (X = P, Si, S, etc.), have also received much attention as cathode material of Li-ion batteries. $LiFePO_4$ and $LiMnO_4$ are of the well-known poly-anionic cathode materials. This could be linked with their great power capability and proper structural stability. Nevertheless, low conductivity of the aforementioned materials has restricted their applications [22][23].

Synthesis of highly efficient cathode materials is considered as a key building block toward progress of energy storage systems with high power and proper capacity in the future. Numerous researchers have illustrated great potential of the electrospun structures as cathode material of the Li-ion batteries. Besides storage capacity, cycling stability is considered as an important parameter for determination of the efficiency and capability of a designed cathode material. Cycling durability is measured by calculation of the storage capacity in various cycles. Apparently, a more ideal battery structure would be obtained through increment of the cycling stability. Commercial LIBs normally show cycling stability during first 300 to 500 cycles (or about 2 to 3 years) [24][25]. As an example, electrospun $LiCoO_2$ fibers (148 $mAh{\cdot}g^{-1}$) result in higher cyclic stability compared with the $LiCoO_2$ powders (138 $mAh{\cdot}g^{-1}$) [26]. Notably, the enhanced capacity of the nanofibrous structures could also be further improved through modification of the electrospun fibers by coating methods. In addition, electrospun LiM_2O_4 structures provide faster diffusion of the lithium ions as well as the promoted cycling stability. In fact, the highly porous structure of the electrospun fibers leads to reduction of the degradation rate during charging/discharging processes [27][28]. Moreover, presence of the carbon nanofibers in the poly-anionic compounds such as $LiFePO_4$ compensates the poor ionic conductivity of this category of cathode materials and causes approaching a more appropriate rate capability [29]. The most recent approaches in fabrication of electrospun fibers applicable as cathode materials are summarized in Table 1.

Table 1. The most recent approaches toward fabrication of nanofibrous cathodes.

Material	Capacity ($mAh{\cdot}g^{-1}$)	Cycling Stability	Autor (Year)	Ref.
$Li_2CoTi_3O_8/TiO_2$	82 at 0.1 C	83% after 25 cycles	Kap et al. (2020)	[30]
$LiFePO_4$ nanocrystals/carbon nanofibers (CNFs)	152 at 0.5 C	98.2% after 500 cycles	Cao et al. (2020)	[31]
V_2O_5/GO	342 at 0.5 C	80% after 20 cycles	Ahmadian et al. (2020)	[32]
Li_2MnTiO_{4+z}	210 at 0.1 C	95.3% after 100 cycles	Vu et al. (2020)	[33]
$LiFe_{0.8}Mn_{0.2}PO_4/C$	169.9 at 0.1 C	160 after 200 cycles	Chen et al. (2020)	[34]

Material	Capacity ($mAh·g^{-1}$)	Cycling Stability	Autor (Year)	Ref.
$LiFe_{0.4}Mn_{0.6}PO_4$/CNFs	133.5 at 1 C	138.8 after 100 cycles	Yang et al. (2020)	[35]

2.2. Electrospun Anode Materials

Intercalation-, conversion-reaction-, and alloying-reaction-based materials are various categories which have been applied as anodes of LIBs. In the intercalation group, the Li^+ ions are placed between the layers of the utilized anode material. Graphite is the most well-known intercalation-based anode structure. In the low voltage range (<0.25 V), high capacity of 360 $mAh·g^{-1}$ along with 100% discharge/charge efficiency have been recorded for this anode structure, whereas most of the electrolyte solvents (e.g., ethylene carbonate (EC), propylene carbonate (PC), and so on) are decomposed between 0.5 and 0.7 V, resulting in the formation of a solid–electrolyte interface (SEI) layer. It is worth noting that proper ionic conductivity, low electrical conductivity, and great stability are the essential characteristics of the ideal SEI layer. Overall, poor capacity is a major drawback associated with the graphite anode materials [36][37].

Surface-to-volume ratio enhancement of the applied anode material is an effective method toward providing more accommodations for the Li^+ ions. Therefore, various studies have been devoted to fabrication of carbonaceous nanomaterials. PAN is the most common precursor for synthesis of electrospun carbon fibers. This could be linked with the simple fabrication procedure, proper mechanical characteristics, and affordable cost. However, environmental concerns associated with DMF, an essential solvent for dissolving PAN polymer, has led to investigation for new precursor resources including lignin, polyvinyl alcohol (PVA), and many more [36][37]. Kim et al. [38] reported a large capacity of 450 $mAh·g^{-1}$ derived from the electrospun PAN nanofibers. In another attempt, Chen et al. [39] introduced a large capacity of 1150 $mAh·g^{-1}$ at 0.1 $A·g^{-1}$ for a hollow CNT/CNF composite. In addition, Culebras et al. [40] claimed a high capacity of 611 $mAh·g^{-1}$ after 500 cycles for a CNF mat obtained from lignin/polylactic acid (PLA) precursor. Moreover, Nan et al. [41] revealed a large capacity of 841 $mAh·g^{-1}$ for a carbon nanofiber membrane synthesized from a PVA precursor. Notably, fabrication of porous and hollow CNFs could result in enhancement of the discharge capacity through increment of the Li^+ ions' spaces. Further, it causes easier interaction between electrode and electrolyte components by reduction of the distances between ions and electronics [42].

Conversion-reaction-based anode materials work based on the faradic reaction. Metal oxides (e.g., Co_3O_4, Cu_2O, etc.), metal nitrides (M_xN_y, where M is Ni, Fe, Mo, etc.), metal sulfides (M_xS_y, where M is Ni, Fe, Mo, etc.), and metal phosphides ($Li_xM_yP_4$, where M is V, Cu, Ti, etc.) are of the conversion-reaction-based structures. These kinds of anode structures are able to provide capacity in the range from 350 $mAh·g^{-1}$ (Cu_2S) to 1800 $mAh·g^{-1}$ (MnP_4). Despite the high capacity, the conversion-reaction-based materials suffer from low potential, poor cycling durability, and high volume changes during extraction and insertion of the Li^+ ions. In order to suppress volume changes of the conversion-reaction-based anode structures, fabrication of porous nanomaterials has received wide attention. Existence of pores in such materials manages the volume changes during

lithiation/dilithiation processes through providing sufficient spaces for extraction and contraction of the applied anode material. In addition, combination of these materials with the carbonaceous structures has been claimed as another effective method for control of the volume changes [36][37]. Zhang et al. [43] reported a large capacity of 835 $mAh{\cdot}g^{-1}$ at 0.2 $A{\cdot}g^{-1}$ after 100 cycles for a Mn_3O_4/CNF composite membrane. In addition, a CoO/CNF three-dimensional mat revealed large discharge capacity of 853.5 $mAh{\cdot}g^{-1}$ after 100 cycles [44]. Moreover, electrospun NiO fibers have exhibited a discharge capacity of 784 $mAh{\cdot}g^{-1}$ at 0.08 $A{\cdot}g^{-1}$ [45].

Alloying-reaction-based materials have been considered as the third category of anode structures. Various metals which are able to be alloyed with lithium (such as Se, S, etc.) are classified in this group. During the charging procedure, lithium ions make an alloy with the applied alloying-reaction-based structures. The aforementioned class of anode structures could reveal various capacities based on the applied alloying metal ranging from 660 $mAh{\cdot}g^{-1}$ (Sb) to 4200 $mAh{\cdot}g^{-1}$ (Si). The major drawback linked with this materials are volume changes during insertion and extraction of the lithium ions, which could be suppressed by size reduction of the applied particles as well as combination with the carbonaceous materials [36][37]. Jang et al. [46] revealed a discharge capacity of 560 $mAh{\cdot}g^{-1}$ after 80 cycles for an electrospun Co-Sn/CNF composite. In addition, a high discharge capacity of 830 $mAh{\cdot}g^{-1}$ at 0.4 $A{\cdot}g^{-1}$ after 100 cycles was claimed for the Si/CNF three dimensional structure [47]. Furthermore, a SnS/CNF composite membrane presented 648 $mAh{\cdot}g^{-1}$ discharge capacity at 0.2 $A{\cdot}g^{-1}$ after 500 cycles [48]. Table 2 describes some of the most recent advancements carried out for the fabrication of highly efficient electrospun anodes.

Table 2. Summarization of some of the most recent approaches toward fabrication of nanofibrous anodes.

Material	Energy Storage Mechanism	Capacity ($mAh{\cdot}g^{-1}$)	Autor (Year)	Ref.
CNF	Intercalation	294 at 0.2 $A{\cdot}g^{-1}$	Li et al. (2020)	[49]
$MnCo_2O_4$	Conversion reaction	701 at 0.5 $A{\cdot}g^{-1}$	Zhu et al. (2020)	[50]
TiO_2/CNF		399	Su et al. (2020)	[51]
Fe_3O_4/CNF		1635 at 1 $A{\cdot}g^{-1}$	Liu et al. (2020)	[52]
Sn_4P_3/CNF	Alloying reaction	710	Ran et al. (2020)	[53]
P/CNF		730 at 0.1 $A{\cdot}g^{-1}$	Liberale et al. (2020)	[54]
Si/PCNF		1033 at 5 $A{\cdot}g^{-1}$	Tian et al. (2020)	[55]
$SnP_{0.94}$/CNF		750 at 0.1 $A{\cdot}g^{-1}$	Yadav et al. (2020)	[56]
SnSe/CNF	Conversion/Alloying reactions	405 at 1 $A{\cdot}g^{-1}$	Xia et al. (2020)	[57]
SnSe/N-doped CNF		460 at 0.2 $A{\cdot}g^{-1}$	Shaji et al. (2020)	[58]

2.3. Electrospun Separator

The separator is another essential key component of LIBs. Prevention of the contact between positive and negative electrodes and transportation of the Li^+ ions between the electrodes, along with retaining the liquid electrolyte are apparent responsibilities of this crucial element. Regarding the role of a separator part in LIBs, an ideal separator must provide sufficient ionic conductivity, wettability, and permeability. In addition, dimensional, thermal, and electrochemical stabilities are other vital characteristics of an appropriate separator. Porous PP or PE membranes are common structures utilized as separators in LIBs. However, poor conductivity as well as low wettability are the most well-known downsides associated with these kinds of separators. Among various techniques applied for the fabrication of ideal separators, electrospun membranes have revealed more appealing features. The highly porous structure of the nanofibrous mats, interconnected pores, and large surface-to-volume ratios of the electrospun fibers provide proper wettability and permeability for separators [59][60].

The electrospun separators are mainly divided into four classes, including: monolayer, multilayer, modified, and composite membranes. Monolayer separators are mainly fabricated from one polymeric precursor such as PVDF [61], polyimide (PI) [62][63], PAN [64][65], and so on, while multilayer membranes are obtained by sequential fabrication of various polymer precursors. In this method, appropriate advantages of the various polymers (such as thermal stability, dimensional stability, electrochemical performance, etc.) could be attained in one separator membrane. PVDF/poly(m-phenylene isophthalamide) (PMIA) [66], PVDF/polyethylene terephthalate (PET) [67], PVDF/PI [68], and polysulfonamide (PSA)/PET [69] are some of the reported multilayer electrospun separators. Post-treatment of the electrospun fibrous membranes is a great technique for modification and improvement of various characteristics. Dip-coating [70][71], in situ polymerization [72][73], and atomic layer deposition [74] are significant modification methods. In such procedures, a material is introduced into the electrospun separator, which results in improvement of its final properties. Direct electrospinning of the combination of two polymer solutions (e.g., PAN/PU [75], PAN/Lignin [76], PSA/PVDF-HFP [77], and so on) or filler-loaded polymer solution (e.g., PAN/SiO_2 [78], PI/Al_2O_3 [79], Nylon6,6/TiO_2 [80], etc.) leads to the fabrication of composite separator membranes with enhanced hydrophilicity and heightened thermal stability. Besides the role of the polymer type, the morphology of the electrospun fibers also influences the obtained electrochemical behavior. As an example, fabrication of finer fibers results in increment of electrolyte uptake and so enhancement of the ionic conductivity. Therefore, the morphology of the electrospun fibers should be tuned to approach appropriate electrospun separators with proper electrochemical characteristics [81]. A summary of the recent progresses in the fabrication of electrospun separators is provided in Table 3.

Table 3. Recent approaches toward fabrication of electrospun separator applicable in Li-ion batteries.

Material	Porosity (%)	Tensile Strength (MPa)	Electrolyte Uptake (%)	Ionic Conductivity ($mS{\cdot}cm^{-1}$)	Autor (Year)	Ref.
PAN	67.7	11.3	478.2	1.97	Dong et al. (2020)	[82]
PAN/PBS	59.3	7.66	665	2.1	Wei et al. (2020)	[83]

Material	Porosity (%)	Tensile Strength (MPa)	Electrolyte Uptake (%)	Ionic Conductivity ($mS \cdot cm^{-1}$)	Autor (Year)	Ref.
PVA/ZrO_2	78	14.5	350	2.19	Xiao et al. (2020)	[84]
PI/Al_2O_3	81	-	912	-	Iaritphun et al. (2020)	[85]
PVDF-HFP/SiO_2	89.7	5	483	-	Xu et al. (2020)	[86]
PVDF-HFP/PI	85.9	9.76	483.5	1.78	Cai et al. (2020)	[87]
PVDF-HFP/LAGP	-	-	215	3.18	Liang et al. (2021)	[88]
PVDF/TPP/CA	90	6.9	301	4.4	Chen et al. (2020)	[89]
PAN/HCNFs@PVDF/UiO-66	77.61	24.77	570.97	1.59	Fa et al. (2021)	[90]

2.4. Electrospun Electrolyte

Cycle life, power density, and safety of LIBs are influenced by their electrolyte elements. In batteries, the electrolyte component transports the Li^+ ions between the electrodes to complete the charge and discharge cycles. In the commercial LIBs, liquid electrolytes, consisting of an organic solvent and a lithium salt, are mainly utilized to fabricate the electrochemical cells. However, flammability of the applied solvents requires metallic sealing for the battery, which results in the production of heavy, inflexible, and expensive cells. Solvent-free electrolytes have been widely recommended as a solution toward fabrication of lightweight, safe, and cost-effective batteries. In such electrochemical cells, the solid electrolyte structure supports the role of both electrolyte and separator. In fact, it prevents the contact between electrodes and transports the Li^+ ions between them. All-solid-state electrolytes are generally synthesized based upon polymeric structures and inorganic solid materials [91][92].

Polymeric solvent-free electrolytes are synthesized based on dispersion of a lithium salt ($LiBF_4$, $LiClO_4$, LiTFSI, etc.) in a polymer matrix (e.g., PAN, PVDF, PEO, poly(methylmethacrylate) (PMMA), etc.). They are mainly fabricated in the formation of casted films. Poor ionic conductivity has been claimed as the main drawback of the polymeric electrolytes. Formation of polymer/salt crystalline phases has been introduced as one of the inhibitor parameters for Li^+ ion movements during cycling processes. In such combinations, Li^+ ions are transported between the electrodes through polymer chain local motions or hopping mechanism. So, reduction of the glass transition temperature as well as increment of the amorphous regions are key solutions for enhancement of the ionic conductivity of the polymer films [92][93]. Therefore, introduction of particulate fillers (such as SiO_2 [94], Al_2O_3 [95], TiO_2 [96], and many more) and plasticizer molecules (such as EC, PC, etc.) into the polymer matrix have

been reported as influential methods for enhancement of the ionic conductivity. Particulate fillers placed between polymer chains of the utilized polymer matrix cause reduction of the crystalline phases. Thus, the polymer chains would be able to move easily and so accelerate transportation of the Li^+ ions. In addition, inserted fillers enhance ion pair dissociation of the applied lithium salts, which obviously influences the ionic conductivity [94][95][96]. In 2017, Freitag et al. reported higher conductivity of the electrospun solvent-free electrolytes in comparison with that of the casted ones. Based on this research, PEO/SN/$LiBF_4$ electrospun electrolyte could exhibit a high ionic conductivity of 0.2 $mS{\cdot}cm^{-1}$ [97]. In a similar research, they showed a high ionic conductivity of 0.1 $mS{\cdot}cm^{-1}$ for the electrospun PEO/SN/$NaBF_4$ membrane [98]. Higher ionic conduction of the solvent-free electrospun structures compared with that of the solution-casted membranes are linked with two main issues. First, small pores between the electrospun fibers are excellent pathways for transportation of the Li^+ ions. Second, fast evaporation of the solvent during electrospinning procedure does not allow the polymer chains and lithium salts to form polymer/salt crystalline regions. So, concentration of the free lithium ions increases in the electrospun membranes, leading to enhancement of the ionic conductivity [4][99]. It is worth noting that electrochemical behavior of the electrospun mats highly depends on the morphology of the fabricated fibers. Based on the obtained results, ionic conductivity could be enhanced by reduction of the average fiber diameter to an optimum range. This may be linked with formation of tiny pores and so more ideal pathways for fast transportation of the Li^+ ions. Nevertheless, further decrement in average diameter of the fabricated fibers could result in reduction of the ionic conductivity. This trend is attributed to formation of more crystalline regions in the structure of finer fibers as well as superior density of the electrospun fibrous mats containing thinner fibers [4][100]. A comparison between ionic conductivity of the electrospun and solution-casted electrolytes with similar chemical compositions is provided in Table 4.

Table 4. Ionic conductivity of the electrospun and solution-casted membranes with similar chemical compositions.

Material	Fabrication Method	Ionic Conductivity ($mS{\cdot}cm^{-1}$)	Author (Year)	Ref.
PEO/PC/$LiClO_4$	Casting	1.7×10^{-3}	Banitaba et al. (2019)	[101]
	Electrospinning	5×10^{-2}		
PEO/Li(TFSI)	Casting	1×10^{-3}	Walk et al. (2018)	[102]
	Electrospinning	4.4×10^{-3}		
PEO/EC/$LiClO_4$	Casting	8×10^{-3}	Banitaba et al. (2020)	[100]
	Electrospinning	1.72×10^{-1}		
PEO/EC/$LiClO_4$/Al_2O_3	Casting	4.4×10^{-3}	Banitaba et al. (2019)	[103]
	Electrospinning	5.9×10^{-2}		

Inorganic solid materials have also been evaluated as applicable all-solid-state electrolyte in the LIB structures. Crystalline structure of such materials facilitates fast migration of the Li^+ ions between the positive and negative

electrodes. Garnet-type, LISICON-like, NASICON-like, and Argyrodite are well-known inorganic solid structures which are able to reveal high ionic conductivity as high as the liquid electrolytes. As an example, lithium germanium phosphorous sulfide ($Li_{10}GeP_2S_{12}$), classified in the LISICON-like category, has shown a high ionic conductivity of 10 $mS{\cdot}cm^{-1}$ at room temperature. Nevertheless, the existence of rare and expensive elements in the structure of inorganic solid materials, along with low flexibility, has restricted their practical usage. To overcome the aforementioned obstacles, several researchers have suggested applying electrospun inorganic solid materials as fillers in the polymeric membranes [104][105][106]. So, a high ionic conductivity of 0.25 $mS{\cdot}cm^{-1}$ has been reported for a PEO-based polymeric membrane incorporated with the electrospun $Li_{6.4}La_3Zr_2Al_{0.2}O_{12}$ fillers [104]. In addition, ionic conductivity of a PAN-based casted film was enhanced up to 0.24 $mS{\cdot}cm^{-1}$ through introduction of $Li_{0.33}La_{0.557}TiO_3$ nanofibers (Figure 3) [105]. Moreover, Liu et al. [106] have reported that dispersion of well-oriented ceramic nanowires instead of random nanowires in a host polymer matrix could cause more ionic conductivity resulting from faster transportation of the Li^+ ions. Hence, morphological features play a key role to obtain ideal electrochemical nanofibrous components.

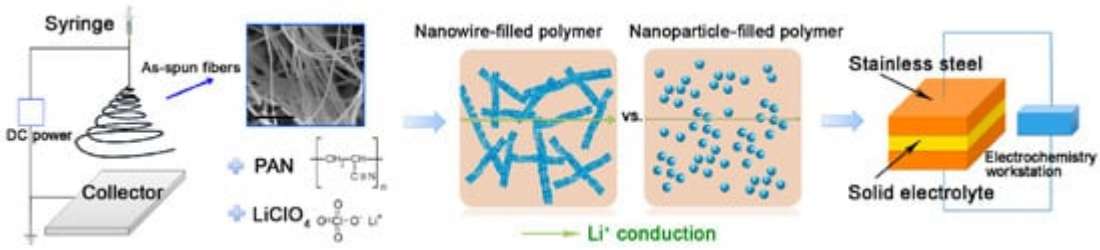

Figure 2. Schematic illustration of the synthesis of ceramic nanowire-filled polymer-based composite electrolytes, together with the comparison of possible lithium-ion conduction pathway in nanowire-filled and nanoparticle-filled composite electrolytes, and illustration of the electrode. Reprinted with permission from [105]. Copyright (2015) American Chemical Society.

So far, lithium secondary batteries have been widely utilized as energy storage devices in various applications. Regarding progress and development of technology, production of storage power tools with superior efficiency and improved function has been crucial. In order to achieve this significant aim, all battery components, including anode, cathode, separator, and electrolyte should be enhanced and augmented. In recent decades, the electrospinning technique has shown a great potential to approach versatile and highly efficient fibrous structures for designing advanced LIBs. Despite the reported advantages of electrospun components of LIBs, several drawbacks, such as poor mechanical strength, low electrical conductivity, and poor ionic conduction, have restricted their practical applications. Meanwhile, such downsides could be eliminated through further evaluation and modification of electrospun membranes. By addressing the mentioned challenges, fabrication of all-solid-state electrospun batteries comprising of nanofibous electrodes along with nanofibrous electrolyte could be considered as the main trend in the near future.

References

1. Haider, A.; Haider, S.; Kang, I.-K. A comprehensive review summarizing the effect of electrospinning parameters and potential applications of nanofibers in biomedical and biotechnology. Arab. J. Chem. 2018, 11, 1165–1188.
2. Ibrahim, H.M.; Klingner, A. A review on electrospun polymeric nanofibers: Production parameters and potential applications. Polym. Test. 2020, 90, 106647.
3. Rodríguez-Tobías, H.; Morales, G.; Grande, D. Comprehensive review on electrospinning techniques as versatile approaches toward antimicrobial biopolymeric composite fibers. Mater. Sci. Eng. C 2019, 101, 306–322.
4. Banitaba, S.N.; Semnani, D.; Heydari-Soureshjani, E.; Rezaei, B.; Ensafi, A.A. The effect of concentration and ratio of ethylene carbonate and propylene carbonate plasticizers on characteristics of the electrospun PEO-based electrolytes applicable in lithium-ion batteries. Solid State Ion. 2020, 347, 115252.
5. Sadek, A.Z.; Baker, C.O.; Powell, D.A.; Wlodarski, W.; Kaner, R.B.; Kalantar-zadeh, K. Polyaniline nanofiber based surface acoustic wave gas sensors—Effect of nanofiber diameter on H2 response. IEEE Sens. J. 2007, 7, 213–218.
6. Şener, A.G.; Altay, A.S.; Altay, F. Effect of voltage on morphology of electrospun nanofibers. In Proceedings of the 2011 7th International Conference on Electrical and Electronics Engineering (ELECO), Bursa, Turkey, 1–4 December 2011; pp. I-324–I-328.
7. Shao, H.; Fang, J.; Wang, H.; Lin, T. Effect of electrospinning parameters and polymer concentrations on mechanical-to-electrical energy conversion of randomly-oriented electrospun poly (vinylidene fluoride) nanofiber mats. RSC Adv. 2015, 5, 14345–14350.
8. Beachley, V.; Wen, X. Effect of electrospinning parameters on the nanofiber diameter and length. Mater. Sci. Eng. C 2009, 29, 663–668.
9. Stachewicz, U.; Szewczyk, P.K.; Kruk, A.; Barber, A.H.; Czyrska-Filemonowicz, A. Pore shape and size dependence on cell growth into electrospun fiber scaffolds for tissue engineering: 2D and 3D analyses using SEM and FIB-SEM tomography. Mater. Sci. Eng. C 2019, 95, 397–408.
10. Tarus, B.; Fadel, N.; Al-Oufy, A.; El-Messiry, M. Effect of polymer concentration on the morphology and mechanical characteristics of electrospun cellulose acetate and poly(vinyl chloride) nanofiber mats. Alex. Eng. J. 2016, 55, 2975–2984.
11. Angammana, C.J.; Jayaram, S.H. Analysis of the effects of solution conductivity on electrospinning process and fiber morphology. IEEE Trans. Ind. Appl. 2011, 47, 1109–1117.
12. Barré, A.; Deguilhem, B.; Grolleau, S.; Gérard, M.; Suard, F.; Riu, D. A review on lithium-ion battery ageing mechanisms and estimations for automotive applications. J. Power Sources 2013, 241, 680–689.

13. Yoshio, M.; Brodd, R.J.; Kozawa, A. Lithium-Ion Batteries; Springer: Berlin/Heidelberg, Germany, 2009; Volume 1.
14. Zhang, X.; Ji, L.; Toprakci, O.; Liang, Y.; Alcoutlabi, M. Electrospun nanofiber-based anodes, cathodes, and separators for advanced lithium-ion batteries. Polym. Rev. 2011, 51, 239–264.
15. Jung, J.-W.; Lee, C.-L.; Yu, S.; Kim, I.-D. Electrospun nanofibers as a platform for advanced secondary batteries: A comprehensive review. J. Mater. Chem. A 2016, 4, 703–750.
16. Banitaba, S.N. Chapter 14—Application of electrospun fibers for the fabrication of high performance all-solid-state fibrous batteries. In Nanosensors and Nanodevices for Smart Multifunctional Textiles; Ehrmann, A., Nguyen, T.A., Nguyen Tri, P., Eds.; Elsevier: Amsterdam, The Netherlands, 2021; pp. 229–244.
17. Fergus, J.W. Recent developments in cathode materials for lithium ion batteries. J. Power Sources 2010, 195, 939–954.
18. Manthiram, A. A reflection on lithium-ion battery cathode chemistry. Nat. Commun. 2020, 11, 1–9.
19. Yu, F.-D.; Que, L.-F.; Xu, C.-Y.; Wang, M.-J.; Sun, G.; Duh, J.-G.; Wang, Z.-B. Dual conductive surface engineering of Li-rich oxides cathode for superior high-energy-density Li-ion batteries. Nano Energy 2019, 59, 527–536.
20. Bao, Y.; Wang, J.; Qian, Y.; Deng, Y.; Yang, X.; Chen, G. An appropriate amount of new spinel phase induced by control synthesis for the improvement of electrochemical performance of Li-rich layered oxide cathode material. Electrochim. Acta 2020, 330, 135240.
21. Shevtsov, A.; Han, H.; Morozov, A.; Carozza, J.C.; Savina, A.A.; Shakhova, I.; Khasanova, N.R.; Antipov, E.V.; Dikarev, E.V.; Abakumov, A.M. Protective Spinel Coating for Li1.17Ni0.17Mn0.50Co0.17O2 Cathode for Li-Ion Batteries through Single-Source Precursor Approach. Nanomaterials 2020, 10, 1870.
22. Gong, Z.; Yang, Y. Recent advances in the research of polyanion-type cathode materials for Li-ion batteries. Energy Environ. Sci. 2011, 4, 3223–3242.
23. Lei, L.; Zhang, B.; Huang, X.-J. A 3.9 V polyanion-type cathode material for Li-ion batteries. Prog. Nat. Sci. Mater. Int. 2011, 21, 211–215.
24. Moshtev, R.; Johnson, B. State of the art of commercial Li ion batteries. J. Power Sources 2000, 91, 86–91.
25. Joho, F.; Rykart, B.; Imhof, R.; Novák, P.; Spahr, M.E.; Monnier, A. Key factors for the cycling stability of graphite intercalation electrodes for lithium-ion batteries. J. Power Sources 1999, 81, 243–247.
26. Ou, Y.; Wen, J.; Xu, H.; Xie, S.; Li, J. Ultrafine LiCoO2 powders derived from electrospun nanofibers for Li-ion batteries. J. Phys. Chem. Solids 2013, 74, 322–327.

27. Sun, K.; Lu, H.-W.; Li, D.; Zeng, W.; Li, Y.-S.; Fu, Z.-W. Electrospun manganese oxides nanofibers electrode for lithium ion batteries. J. Inorg. Mater. 2009, 24, 357–360.
28. Lu, H.-W.; Zeng, W.; Li, Y.-S.; Fu, Z.-W. Fabrication and electrochemical properties of three-dimensional net architectures of anatase TiO2 and spinel Li4Ti5O12 nanofibers. J. Power Sources 2007, 164, 874–879.
29. Jin, E.M.; Gu, H.-B. Synthesis and electrochemical properties of LiFePO4-graphite nanofiber composites as cathode materials for lithium ion batteries. J. Power Sources 2013, 244, 586–591.
30. Kap, Ö.; Inan, A.; Er, M.; Horzum, N. Li-ion battery cathode performance from the electrospun binary LiCoO2 to ternary Li2CoTi3O8. J. Mater. Sci. Mater. Electron. 2020, 31, 8394–8402.
31. Cao, Z.; Sang, M.; Chen, S.; Jia, J.; Yang, M.; Zhang, H.; Li, X.; Yang, S. In situ constructed (010)-oriented LiFePO4 nanocrystals/carbon nanofiber hybrid network: Facile synthesis of free-standing cathodes for lithium-ion batteries. Electrochim. Acta 2020, 333, 135538.
32. Ahmadian, A. Design and Fabrication of High Capacity Lithium-Ion Batteries Using Electro-Spun Graphene Modified Vanadium Pentoxide Cathodes. Ph.D. Thesis, Purdue University Graduate School, West Lafayette, IN, USA, 2020.
33. Vu, N.H.; Dao, V.-D.; Van, H.N.; Huy, L.T.; Quang, N.T.; Huu, H.T.; Choi, S.; Im, W.B. Spinel-layered Li2MnTiO4+z nanofibers as cathode materials for Li-ion batteries. Solid State Sci. 2020, 103, 106178.
34. Chen, W.; Xu, D.; Chen, Y.; Tang, T.; Kuang, S.; Fu, H.; Zhou, W.; Yu, X. In situ electrospinning synthesis of N-doped C nanofibers with uniform embedding of Mn doped MFe1−xMnxPO4 (M= Li, Na) as a High Performance Cathode for Lithium/Sodium-Ion Batteries. Adv. Mater. Interfaces 2020, 7, 2000684.
35. Yang, J.; Tan, R.; Li, D.; Ma, J.; Duan, X. Ionic liquid-assisted electrospinning of porous LiFe0.4Mn0 6PO4/CNFs as free-standing cathodes with pseudocapacitive contribution for high-performance lithium-ion batteries. Chem. A Eur. J. 2020, 26, 5341–5346.
36. Zeng, S.; Zhao, R.; Li, A.; Xue, S.; Lv, D.; Luo, Q.; Shu, D.; Chen, H. MnO/Carbon fibers prepared by an electrospinning method and their properties used as anodes for lithium ion batteries. Appl. Surf. Sci. 2019, 463, 211–216.
37. Ma, X.; Smirnova, A.L.; Fong, H. Flexible lignin-derived carbon nanofiber substrates functionalized with iron (III) oxide nanoparticles as lithium-ion battery anodes. Mater. Sci. Eng. B 2019, 241, 100–104.
38. Kim, C.; Yang, K.S.; Kojima, M.; Yoshida, K.; Kim, Y.J.; Kim, Y.A.; Endo, M. Fabrication of electrospinning-derived carbon nanofiber webs for the anode material of lithium-ion secondary batteries. Adv. Funct. Mater. 2006, 16, 2393–2397.

39. Chen, Y.; Li, X.; Park, K.; Song, J.; Hong, J.; Zhou, L.; Mai, Y.-W.; Huang, H.; Goodenough, J.B. Hollow Carbon-Nanotube/Carbon-Nanofiber Hybrid Anodes for Li-Ion Batteries. J. Am. Chem. Soc. 2013, 135, 16280–16283.
40. Culebras, M.; Geaney, H.; Beaucamp, A.; Upadhyaya, P.; Dalton, E.D.; Ryan, K.M.; Collins, M.N. Bio-derived carbon nanofibers from lignin as high performance Li-ion anode materials. ChemSusChem 2019, 12, 1–7.
41. Nan, D.; Huang, Z.-H.; Lv, R.; Lin, Y.; Yang, L.; Yu, X.; Ye, L.; Shen, W.; Sun, H.; Kang, F. Silicon-encapsulated hollow carbon nanofiber networks as binder-free anodes for lithium ion battery. J. Nanomater. 2014, 2014, 139639.
42. Peng, Y.-T.; Lo, C.-T. Electrospun porous carbon nanofibers as lithium ion battery anodes. J. Solid State Electrochem. 2015, 19, 3401–3410.
43. Zhang, D.; Li, G.; Fan, J.; Li, B.; Li, L. In Situ Synthesis of Mn3O4 nanoparticles on hollow carbon nanofiber as high-performance lithium-ion battery anode. Chem. A Eur. J. 2018, 24, 9632–9638.
44. Ryu, W.-H.; Shin, J.; Jung, J.-W.; Kim, I.-D. Cobalt(ii) monoxide nanoparticles embedded in porous carbon nanofibers as a highly reversible conversion reaction anode for Li-ion batteries. J. Mater. Chem. A 2013, 1, 3239–3243.
45. Aravindan, V.; Suresh Kumar, P.; Sundaramurthy, J.; Ling, W.C.; Ramakrishna, S.; Madhavi, S. Electrospun NiO nanofibers as high performance anode material for Li-ion batteries. J. Power Sources 2013, 227, 284–290.
46. Jang, B.-O.; Park, S.-H.; Lee, W.-J. Electrospun Co–Sn alloy/carbon nanofibers composite anode for lithium ion batteries. J. Alloys Compd. 2013, 574, 325–330.
47. Jiang, Y.; Chen, S.; Mu, D.; Wu, B.; Liu, Q.; Zhao, Z.; Wu, F. A three-dimensional network structure Si/C anode for Li-ion batteries. J. Mater. Sci. 2017, 52, 10950–10958.
48. Xia, J.; Liu, L.; Jamil, S.; Xie, J.; Yan, H.; Yuan, Y.; Zhang, Y.; Nie, S.; Pan, J.; Wang, X.; et al. Free-standing SnS/C nanofiber anodes for ultralong cycle-life lithium-ion batteries and sodium-ion batteries. Energy Storage Mater. 2019, 17, 1–11.
49. Li, X.; Sun, N.; Tian, X.; Yang, T.; Song, Y.; Xu, B.; Liu, Z. Electrospun coal liquefaction residues/polyacrylonitrile composite carbon nanofiber nonwoven fabrics as high-performance electrodes for lithium/potassium batteries. Energy Fuels 2020, 34, 2445–2451.
50. Zhu, L.; Li, F.; Yao, T.; Liu, T.; Wang, J.; Li, Y.; Lu, H.; Qian, R.; Liu, Y.; Wang, H. Electrospun MnCo2O4 nanotubes as high-performance anode materials for lithium-ion batteries. Energy Fuels 2020, 34, 11574–11580.
51. Su, D.; Liu, L.; Liu, Z.; Dai, J.; Wen, J.; Yang, M.; Jamil, S.; Deng, H.; Cao, G.; Wang, X. Electrospun Ta-doped TiO2/C nanofibers as a high-capacity and long-cycling anode material for

Li-ion and K-ion batteries. J. Mater. Chem. A 2020, 8, 20666–20676.

52. Liu, Y.; Chen, J.; Liu, Z.; Xu, H.; Zheng, Y.; Zhong, J.; Yang, Q.; Tian, H.; Shi, Z.; Yao, J.; et al. Facile fabrication of Fe3O4 nanoparticle/carbon nanofiber aerogel from Fe-ion cross-linked cellulose nanofibrils as anode for lithium-ion battery with superhigh capacity. J. Alloys Compd. 2020, 829, 154541.
53. Ran, L.; Gentle, I.; Lin, T.; Luo, B.; Mo, N.; Rana, M.; Li, M.; Wang, L.; Knibbe, R. Sn4P3@Porous carbon nanofiber as a self-supported anode for sodium-ion batteries. J. Power Sources 2020, 461, 228116.
54. Liberale, F.; Fiore, M.; Ruffo, R.; Bernasconi, R.; Shiratori, S.; Magagnin, L. Red phosphorus decorated electrospun carbon anodes for high efficiency lithium ion batteries. Sci. Rep. 2020, 10, 13233.
55. Tian, X.; Xu, Q.; Cheng, L.; Meng, L.; Zhang, H.; Jia, X.; Bai, S.; Qin, Y. Enhancing the performance of a self-standing si/pcnf anode by optimizing the porous structure. ACS Appl. Mater. Interfaces 2020, 12, 27219–27225.
56. Yadav, P.; Malik, W.; Dwivedi, P.K.; Jones, L.A.; Shelke, M.V. Electrospun nanofibers of tin phosphide (SnP0.94) nanoparticles encapsulated in a carbon matrix: A tunable conversion-cum-alloying lithium storage anode. Energy Fuels 2020, 34, 7648–7657.
57. Xia, J.; Yuan, Y.; Yan, H.; Liu, J.; Zhang, Y.; Liu, L.; Zhang, S.; Li, W.; Yang, X.; Shu, H.; et al. Electrospun SnSe/C nanofibers as binder-free anode for lithium–ion and sodium-ion batteries. J. Power Sources 2020, 449, 227559.
58. Shaji, N.; Santhoshkumar, P.; Kang, H.S.; Nanthagopal, M.; Park, J.W.; Praveen, S.; Sim, G.S.; Senthil, C.; Lee, C.W. Tin selenide/N-doped carbon composite as a conversion and alloying type anode for sodium-ion batteries. J. Alloys Compd. 2020, 834, 154304.
59. Cho, T.-H.; Tanaka, M.; Ohnishi, H.; Kondo, Y.; Yoshikazu, M.; Nakamura, T.; Sakai, T. Composite nonwoven separator for lithium-ion battery: Development and characterization. J. Power Sources 2010, 195, 4272–4277.
60. Hao, J.; Lei, G.; Li, Z.; Wu, L.; Xiao, Q.; Wang, L. A novel polyethylene terephthalate nonwoven separator based on electrospinning technique for lithium ion battery. J. Membr. Sci. 2013, 428, 11–16.
61. Liang, Y.; Cheng, S.; Zhao, J.; Zhang, C.; Sun, S.; Zhou, N.; Qiu, Y.; Zhang, X. Heat treatment of electrospun Polyvinylidene fluoride fibrous membrane separators for rechargeable lithium-ion batteries. J. Power Sources 2013, 240, 204–211.
62. Cao, L.; An, P.; Xu, Z.; Huang, J. Performance evaluation of electrospun polyimide non-woven separators for high power lithium-ion batteries. J. Electroanal. Chem. 2016, 767, 34–39.

63. Jiang, W.; Liu, Z.; Kong, Q.; Yao, J.; Zhang, C.; Han, P.; Cui, G. A high temperature operating nanofibrous polyimide separator in Li-ion battery. Solid State Ion. 2013, 232, 44–48.
64. Cho, T.-H.; Tanaka, M.; Onishi, H.; Kondo, Y.; Nakamura, T.; Yamazaki, H.; Tanase, S.; Sakai, T. Battery performances and thermal stability of polyacrylonitrile nano-fiber-based nonwoven separators for Li-ion battery. J. Power Sources 2008, 181, 155–160.
65. Evans, T.; Lee, J.-H.; Bhat, V.; Lee, S.-H. Electrospun polyacrylonitrile microfiber separators for ionic liquid electrolytes in Li-ion batteries. J. Power Sources 2015, 292, 1–6.
66. Zhai, Y.; Wang, N.; Mao, X.; Si, Y.; Yu, J.; Al-Deyab, S.S.; El-Newehy, M.; Ding, B. Sandwich-structured PVdF/PMIA/PVdF nanofibrous separators with robust mechanical strength and thermal stability for lithium ion batteries. J. Mater. Chem. A 2014, 2, 14511–14518.
67. Zhu, C.; Nagaishi, T.; Shi, J.; Lee, H.; Wong, P.Y.; Sui, J.; Hyodo, K.; Kim, I.S. Enhanced wettability and thermal stability of a novel polyethylene terephthalate-based poly(vinylidene fluoride) nanofiber hybrid membrane for the separator of lithium-ion batteries. ACS Appl. Mater. Interfaces 2017, 9, 26400–26406.
68. Wu, D.; Shi, C.; Huang, S.; Qiu, X.; Wang, H.; Zhan, Z.; Zhang, P.; Zhao, J.; Sun, D.; Lin, L. Electrospun nanofibers for sandwiched polyimide/poly (vinylidene fluoride)/polyimide separators with the thermal shutdown function. Electrochim. Acta 2015, 176, 727–734.
69. Peng, K.; Wang, B.; Ji, C. A poly(ethylene terephthalate) nonwoven sandwiched electrospun polysulfonamide fibrous separator for rechargeable lithium ion batteries. J. Appl. Polym. Sci. 2017, 134, 44907.
70. Cao, C.; Tan, L.; Liu, W.; Ma, J.; Li, L. Polydopamine coated electrospun poly(vinyldiene fluoride) nanofibrous membrane as separator for lithium-ion batteries. J. Power Sources 2014, 248, 224–229.
71. Shi, C.; Dai, J.; Huang, S.; Li, C.; Shen, X.; Zhang, P.; Wu, D.; Sun, D.; Zhao, J. A simple method to prepare a polydopamine modified core-shell structure composite separator for application in high-safety lithium-ion batteries. J. Membr. Sci. 2016, 518, 168–177.
72. Park, S.-R.; Jung, Y.-C.; Shin, W.-K.; Ahn, K.H.; Lee, C.H.; Kim, D.-W. Cross-linked fibrous composite separator for high performance lithium-ion batteries with enhanced safety. J. Membr. Sci. 2017, 527, 129–136.
73. Ye, W.; Zhu, J.; Liao, X.; Jiang, S.; Li, Y.; Fang, H.; Hou, H. Hierarchical three-dimensional micro/nano-architecture of polyaniline nanowires wrapped-on polyimide nanofibers for high performance lithium-ion battery separators. J. Power Sources 2015, 299, 417–424.
74. Shen, X.; Li, C.; Shi, C.; Yang, C.; Deng, L.; Zhang, W.; Peng, L.; Dai, J.; Wu, D.; Zhang, P.; et al. Core-shell structured ceramic nonwoven separators by atomic layer deposition for safe lithium-ion batteries. Appl. Surf. Sci. 2018, 441, 165–173.

75. Zainab, G.; Wang, X.; Yu, J.; Zhai, Y.; Ahmed Babar, A.; Xiao, K.; Ding, B. Electrospun polyacrylonitrile/polyurethane composite nanofibrous separator with electrochemical performance for high power lithium ion batteries. Mater. Chem. Phys. 2016, 182, 308–314.
76. Zhao, M.; Wang, J.; Chong, C.; Yu, X.; Wang, L.; Shi, Z. An electrospun lignin/polyacrylonitrile nonwoven composite separator with high porosity and thermal stability for lithium-ion batteries. RSC Adv. 2015, 5, 101115–101120.
77. Zhou, X.; Yue, L.; Zhang, J.; Kong, Q.; Liu, Z.; Yao, J.; Cui, G. A core-shell structured polysulfonamide-based composite nonwoven towards high power lithium ion battery separator. J. Electrochem. Soc. 2013, 160, A1341.
78. Yanilmaz, M.; Lu, Y.; Zhu, J.; Zhang, X. Silica/polyacrylonitrile hybrid nanofiber membrane separators via sol-gel and electrospinning techniques for lithium-ion batteries. J. Power Sources 2016, 313, 205–212.
79. Shayapat, J.; Chung, O.H.; Park, J.S. Electrospun polyimide-composite separator for lithium-ion batteries. Electrochim. Acta 2015, 170, 110–121.
80. Yanilmaz, M.; Zhu, J.; Lu, Y.; Ge, Y.; Zhang, X. High-strength, thermally stable nylon 6,6 composite nanofiber separators for lithium-ion batteries. J. Mater. Sci. 2017, 52, 5232–5241.
81. Ma, X.; Kolla, P.; Yang, R.; Wang, Z.; Zhao, Y.; Smirnova, A.L.; Fong, H. Electrospun polyacrylonitrile nanofibrous membranes with varied fiber diameters and different membrane porosities as lithium-ion battery separators. Electrochim. Acta 2017, 236, 417–423.
82. Dong, T.; Arifeen, W.U.; Choi, J.; Yoo, K.; Ko, T. Surface-modified electrospun polyacrylonitrile nano-membrane for a lithium-ion battery separator based on phase separation mechanism. Chem. Eng. J. 2020, 398, 125646.
83. Wei, Z.; Gu, J.; Zhang, F.; Pan, Z.; Zhao, Y. Core–Shell Structured Nanofibers for Lithium Ion Battery Separator with Wide Shutdown Temperature Window and Stable Electrochemical Performance. ACS Appl. Polym. Mater. 2020, 2, 1989–1996.
84. Xiao, W.; Song, J.; Huang, L.; Yang, Z.; Qiao, Q. PVA-ZrO2 multilayer composite separator with enhanced electrolyte property and mechanical strength for lithium-ion batteries. Ceram. Int. 2020, 46, 29212–29221.
85. Jaritphun, S.; Park, J.S.; Chung, O.H.; Nguyen, T.T.T. Sandwiched polyimide-composite separator for lithium-ion batteries via electrospinning and electrospraying. Polym. Compos. 2020, 41, 4478–4488.
86. Xu, Y.; Zhu, J.-W.; Fang, J.-B.; Li, X.; Yu, M.; Long, Y.-Z. Electrospun high-thermal-resistant inorganic composite nonwoven as lithium-ion battery separator. J. Nanomater. 2020, 2020, 3879040.

87. Cai, M.; Yuan, D.; Zhang, X.; Pu, Y.; Liu, X.; He, H.; Zhang, L.; Ning, X. Lithium ion battery separator with improved performance via side-by-side bicomponent electrospinning of PVDF-HFP/PI followed by 3D thermal crosslinking. J. Power Sources 2020, 461, 228123.
88. Liang, T.; Liang, W.-H.; Cao, J.-H.; Wu, D.-Y. Enhanced performance of high energy density lithium metal battery with PVDF-HFP/LAGP composite separator. ACS Appl. Energy Mater. 2021, 4, 2578–2585.
89. Chen, Y.; Qiu, L.; Ma, X.; Dong, L.; Jin, Z.; Xia, G.; Du, P.; Xiong, J. Electrospun cellulose polymer nanofiber membrane with flame resistance properties for lithium-ion batteries. Carbohydr. Polym. 2020, 234, 115907.
90. Fu, Q.; Zhang, W.; Muhammad, I.P.; Chen, X.; Zeng, Y.; Wang, B.; Zhang, S. Coaxially electrospun PAN//UiO-66 composite separator with high strength and thermal stability for lithium-ion battery. Microporous Mesoporous Mater. 2021, 311, 110724.
91. Long, L.; Wang, S.; Xiao, M.; Meng, Y. Polymer electrolytes for lithium polymer batteries. J. Mater. Chem. A 2016, 4, 10038–10069.
92. Murata, K.; Izuchi, S.; Yoshihisa, Y. An overview of the research and development of solid polymer electrolyte batteries. Electrochim. Acta 2000, 45, 1501–1508.
93. Wang, F.; Li, L.; Yang, X.; You, J.; Xu, Y.; Wang, H.; Ma, Y.; Gao, G. Influence of additives in a PVDF-based solid polymer electrolyte on conductivity and Li-ion battery performance. Sustain. Energy Fuels 2018, 2, 492–498.
94. Kim, J.-W.; Ji, K.-S.; Lee, J.-P.; Park, J.-W. Electrochemical characteristics of two types of PEO-based composite electrolyte with functional SiO2. J. Power Sources 2003, 119, 415–421.
95. Joge, P.N.; Kanchan, D.; Sharma, P.L. Effect of Al2O3 on crystallinity and conductivity of PVA-PEO-EC-LiCF3SO3 blend electrolyte system. AIP Conf. Proc. 2014, 1591, 356.
96. Abdel-Samiea, B.; Basyouni, A.; Khalil, R.; Sheha, E.M.; Tsuda, H.; Matsui, T. The role of TiO2 anatase nano-filler to enhance the physical and electrochemical properties of PVA-based polymer electrolyte for magnesium battery applications. J. Mater. Sci. Eng. A 2013, 3, 678–689.
97. Freitag, K.M.; Kirchhain, H.; Wullen, L.V.; Nilges, T. Enhancement of Li ion conductivity by electrospun polymer fibers and direct fabrication of solvent-free separator membranes for Li ion batteries. Inorg. Chem. 2017, 56, 2100–2107.
98. Freitag, K.; Walke, P.; Nilges, T.; Kirchhain, H.; Spranger, R.; van Wüllen, L. Electrospun sodiumtetrafluoroborate-polyethylene oxide membranes for solvent-free sodium ion transport in solid state sodium ion batteries. J. Power Sources 2018, 378, 610–617.
99. Banitaba, S.N.; Semnani, D.; Fakhrali, A.; Ebadi, S.V.; Heydari-Soureshjani, E.; Rezaei, B.; Ensafi, A.A. Electrospun PEO nanofibrous membrane enabled by LiCl, LiClO4, and LiTFSI salts:

A versatile solvent-free electrolyte for lithium-ion battery application. Ionics 2020, 26, 3249–3260.

100. Banitaba, S.N.; Semnani, D.; Heydari-Soureshjani, E.; Rezaei, B.; Ensafi, A.A.; Taghipour-Jahromi, A. Novel electrospun polymer electrolytes incorporated with Keggin-type hetero polyoxometalate fillers as solvent-free electrolytes for lithium ion batteries. Polym. Int. 2020, 69, 675–687.
101. Banitaba, S.N.; Semnani, D.; Rezaei, B.; Ensafi, A.A. Morphology and electrochemical and mechanical properties of polyethy lene-oxide-based nanofibrous electrolytes applicable in lithium ion batteries. Polym. Int. 2019, 68, 746–754.
102. Walke, P.; Freitag, K.M.; Kirchhain, H.; Kaiser, M.; van Wüllen, L.; Nilges, T. Electrospun Li (TFSI)@polyethylene oxide membranes as solid electrolytes. Z. Für Anorg. Und Allg. Chem. 2018, 644, 1863–1874.
103. Banitaba, S.N.; Semnani, D.; Heydari-Soureshjani, E.; Rezaei, B.; Ensafi, A.A. Electrospun Polyethylene Oxide-Based Membranes Incorporated with Silicon Dioxide, Aluminum Oxide and Clay Nanoparticles as Flexible Solvent-Free Electrolytes for Lithium-Ion Batteries. JOM 2019, 71, 4537–4546.
104. Fu, K.K.; Gong, Y.; Dai, J.; Gong, A.; Han, X.; Yao, Y.; Wang, C.; Wang, Y.; Chen, Y.; Yan, C. Flexible, solid-state, ion-conducting membrane with 3D garnet nanofiber networks for lithium batteries. Proc. Natl. Acad. Sci. USA 2016, 113, 7094–7099.
105. Liu, W.; Liu, N.; Sun, J.; Hsu, P.-C.; Li, Y.; Lee, H.-W.; Cui, Y. Ionic conductivity enhancement of polymer electrolytes with ceramic nanowire fillers. Nano Lett. 2015, 15, 2740–2745.
106. Liu, W.; Lee, S.W.; Lin, D.; Shi, F.; Wang, S.; Sendek, A.D.; Cui, Y. Enhancing ionic conductivity in composite polymer electrolytes with well-aligned ceramic nanowire. Nat. Energy 2017, 2, 1–7.